MEK-ERK Pathway Modulation Ameliorates Pulmonary Fibrosis Associated with Epidermal Growth Factor Receptor Activation

Satish K. Madala[1], Stephanie Schmidt[1], Cynthia Davidson[1], Machiko Ikegami[2], Susan Wert[2], and William D. Hardie[1]

[1]Divisions of Pulmonary Medicine and [2]Pulmonary Biology, Cincinnati Children's Hospital Medical Center, Cincinnati, Ohio

Pulmonary fibrosis remains a significant public health burden with no proven therapies. The mitogen-activated protein kinase (MAPK)/MAPK kinase (MEK)/extracellular signal–regulated kinase (ERK) signaling cascade is a major pathway controlling cellular processes associated with fibrogenesis, including growth, proliferation, and survival. Activation of the MAPK/ERK pathway is detected in the lungs of human fibrosis samples; however, the effect of modulating the pathway *in vivo* is unknown. Overexpression of transforming growth factor (TGF)-α in the lung epithelium of transgenic mice causes a progressive pulmonary fibrosis associated with increased MEK/ERK activation localized primarily in mesenchymal cells. To determine the role of the MEK pathway in the induction of TGF-α–induced lung fibrosis, TGF-α was overexpressed for 4 weeks while mice were simultaneously treated with the specific MEK inhibitor, ARRY-142886 (ARRY). Treatment with ARRY prevented increases in lung cell proliferation and total lung collagen, attenuated production of extracellular matrix genes, and protected mice from changes in lung function. ARRY administered as a rescue treatment after fibrosis was already established inhibited fibrosis progression, as assessed by lung histology, changes in body weights, extracellular matrix gene expression, and lung mechanics. These findings demonstrate that MEK inhibition prevents progression of established fibrosis in the TGF-α model, and provides proof of concept of targeting the MEK pathway in fibrotic lung disease.

Keywords: pulmonary fibrosis; transforming growth factor-α; epidermal growth factor receptor; mitogen-activated protein kinase/mitogen-activated protein kinase kinase/extracellular signal–regulated kinase; ARRY-142886

Pulmonary fibrosis is a progressive and often fatal condition characterized pathologically by mesenchymal cell proliferation and differentiation in the lung, expansion of the extracellular matrix, and remodeling of the lung parenchyma and airways (1, 2). Lung fibrosis develops in a number of clinical diseases, including interstitial lung diseases and idiopathic interstitial pneumonias, as part of several systemic connective tissue diseases and childhood interstitial lung disease syndromes, and in response to many types of lung injury, including radiation and some chemotherapeutic drugs (2–4). Initial therapies focused on aggressive anti-inflammatory treatment; however, this approach has not improved loss of lung function or survival (5). Currently, there are no approved medical antifibrotic therapies for pulmonary

CLINICAL RELEVANCE

This study demonstrates mitogen-activated protein kinase kinase (MEK) inhibition prevents the progression of established fibrosis in the transforming growth factor-α model. Previous work has demonstrated activation of the MEK pathway in human fibrotic disease, and findings from this study provides proof of concept of pharmacologic targeting of the MEK pathway in fibrotic lung disease.

fibrosis (5, 6). Over the past decade, substantial progress has been made in understanding the pathophysiology of lung fibrosis, including evidence that inflammation is not required for the development of the fibrotic response, which may account for the observed therapeutic failures (6). Successful antifibrotic therapy may need to focus on mechanisms or pathways downstream of inflammation that mediate fibroproliferation. Previous studies have identified a number of chemokines, cytokines, and growth factors mediating pulmonary fibrosis (7–12). The identification of intracellular signaling pathways eliciting the cellular response of mesenchymal cell proliferation, differentiation, and extracellular matrix deposition may facilitate development of novel therapeutic approaches to ameliorate the global burden of fibroproliferative disease (4, 13, 14).

The epidermal growth factor (EGF) receptor (EGFR; HER1) belongs to a receptor tyrosine kinase protein family that consists of four receptor tyrosine kinases: EGFR (HER1), ERBB2 (also called HER2/neu), ERBB3 (also called HER3), and ERBB4 (also called HER4). All of these, except HER3, have tyrosine kinase activity. Binding of secreted growth factors, such as the EGF and other EGF-like growth factors, including transforming growth factor (TGF)-α and epiregulin, induces receptor dimerization, resulting in the phosphorylation of tyrosine residues in the kinase domain (15–17). Activation of the EGFR has been shown to regulate diverse cellular functions, many of which are associated with fibrogenesis, including cell growth, proliferation, differentiation, migration, survival, and transformation (14, 18). Increases in the EGFR pathway have been associated with a number of human fibrotic diseases (1, 19, 20). Moreover, EGFR is activated both directly and indirectly by several agents, including cytomegalovirus, endotoxin, TNF-α, and IL-13 (21–23). We previously generated doxycycline (Dox)-regulatable transgenic mice wherein lung epithelial–specific expression of TGF-α caused progressive pulmonary fibrosis (7). Pulmonary fibrosis in this transgenic model is characterized by a number of specific phenotypes that are observed in human fibrotic disease, including epithelial and mesenchymal proliferation with myofibroblast transformation, extracellular matrix deposition, severe restrictive changes in lung mechanics, and secondary pulmonary hypertension (18, 24). Moreover, fibrosis develops and progresses in the absence of detectable inflammation, demonstrating that EGFR activation in the lung is a downstream event in pulmonary

fibrosis. Importantly, the TGF-α transgenic mouse is a powerful model for identifying the biologic and molecular mechanisms of pulmonary fibrosis and testing strategies to reverse established and progressive disease (18).

EGFR activates multiple downstream effecter pathways, including the mitogen-activated protein kinase (MAPK)/extracellular signal–regulated kinase cascade (ERK), the janus kinase–signal transducer and activator of transcription pathway, and phosphatidylinositol 3-kinase (PI3K)/Akt/mammalian target of rapamycin (mTOR) 1 signaling pathway (14, 25). A recent study from our laboratory demonstrated that TGF-α–induced pulmonary fibrosis is associated with activation of the PI3K and mTORC1 pathways (18, 26). However, inhibition of PI3K or mTOR1 was not sufficient for a complete reversal of established and progressive fibrosis, suggesting that alternative pathways may contribute to the maintenance of fibrosis (18).

MAPK has been shown to control cellular processes associated with fibrosis, including cell growth, proliferation, migration, protection from apoptosis, and myofibroblast transformation (27, 28). To date, there have been no studies examining the efficacy of ERK1/2 inhibition in reversal of progressive fibrotic disease. However, the recent development of potent, highly specific, allosteric inhibitors of MAPK kinase (MEK) allows the precise dissection of the contributions of the MAPK/ERK pathway in the development and progression of fibrogenesis (29). The purpose of this study was to determine if ERK1/2 is activated during the progression of lung fibrosis in the TGF-α model and identify the cellular distribution. A second goal was to examine the contribution of ERK1/2 activation in mediating lung fibrosis *in vivo* by administering TGF-α transgenic mice the allosteric MEK inhibitor, ARRY-142886 (ARRY), during the initiation of fibrosis as well as a rescue therapy when fibrosis was already established.

MATERIALS AND METHODS

Transgenic Mice and Administration of ARRY

All mice were derived from the FVB/NJ inbred strain. TGF-α transgenic mice were generated and maintained as described previously (7, 30). Single transgenic Clara cell–specific protein (CCSP)-rtTA$^{+/-}$ (abbreviated as CCSP/-) mice and bitransgenic CCSP-rtTA$^{+/-}$/(TetO)$_7$-cmv TGF-α$^{+/-}$ (abbreviated as CCSP/TGF-α) mice were produced within the same litter by mating homozygous CCSP/- mice to hemizygous (TetO)$_7$-cmv TGF-α$^{+/-}$ mice. All mice were housed under specific pathogen–free conditions and protocols were approved by the Institutional Animal Care and Use Committee of the Cincinnati Children's Hospital Research Foundation. To induce TGF-α expression, Dox (Sigma-Aldrich, St. Louis, MO) was administered in food (62.5 mg/kg).

Stock solutions of AZD6244 (ARRY) were prepared in 0.5% methocellulose/0.4% Tween 80. Mice were anesthetized (Isoflurane; Abbott Labs, Chicago, IL), and sterile vehicle or ARRY was administered by gavage using a 20-gauge feeding catheter (Harvard Apparatus, Holliston, MA). Dosing throughout the study was based on original baseline weights, and not adjusted for weight changes. Mice were treated with vehicle or ARRY twice daily for up to 4 weeks.

Fluorescence Microscopy

Lungs were harvested from CCSP/TGF-α and CCSP/- mice treated with Dox for 4 or 28 days and embedded in OCT medium (Tissue-Tek; Sakura Finetek USA, Torrance, CA) for cryosectioning at 6 μm in thickness. Sections were immunostained as described previously (31). In brief, lung sections were blocked at room temperature for 1–2 hours with 3% normal goat or donkey sera. Primary antibodies used for staining included anti-phosphoERK1/2 (Thr202/Tyr204, 1:500; Cell Signaling Technology, Danvers, MA), anti-α-smooth muscle actin (α-SMA) (clone 1A4, 1:500; Sigma-Aldrich), anti-CCSP (sc-9772, 1:500; Santa Cruz Biotechnology, Santa Cruz, CA), anti-vimentin (clone 3B4, 1:250; Millipore, Billerica, MA), and appropriate secondary antibodies (1:1,000 dilution) conjugated with Alexa488 or Alexa647 (Life Technologies, Grand Island, NY). Staining controls included lung sections stained with secondary antibody conjugated with Alexa488 or Alexa647. Image exposures were held constant to reflect changes in staining intensities. Images were pseudocolored on a Zeiss Axioplan2 microscope equipped with AxioVision Software (Zeiss, Thornwood, NY) and analyzed using Adobe Photoshop version 7.0 (Adobe Systems Inc., San Jose, CA).

Mouse and Human Fibroblast Cultures

Mouse primary fibroblasts were generated by culturing the lungs of CCSP/- mice for 10 days as described previously (32). For signaling studies using Western blots, mouse primary fibroblasts were seeded at 0.5 million cells per well using 1% FBS containing Dulbecco's modified Eagle's medium in 12-well plates. After 12 hours of resting, fibroblasts were pretreated for 30 minutes with 0.1, 5, and 10 μM of ARRY in DMSO. Final concentration of DMSO in cultures was less than 0.1%, and no effect of DMSO was observed on signaling or viability of fibroblasts. Control or ARRY-added cells were treated with or without TGF-α (10 ng/ml; R&D Systems, Minneapolis, MN). After 30 minutes of treatment, media were removed and cell lysates were prepared for Western blot analysis in RIPA buffer (Santa Cruz Biotechnology, Santa Cruz, CA).

Normal human fibroblasts derived from lungs, ALF CCD-19 Lu (CCL-210; ATCC, Manassas, VA), were cultured in 10% FBS Dulbecco's modified Eagle's medium (Invitrogen). Cells were seeded and treated with ARRY and/or TGF-α as described previously here for mouse primary fibroblasts.

Western Blots

Western blot analysis was performed on lung homogenates and lung fibroblast lysates from culture, and quantified using the volume integration function on PhosphorImager software Imagequant 5.2 (Molecular Dynamics, Piscataway, NJ), as previously described (26). Primary antibodies used included anti–glyceraldehyde 3-phosphate dehydrogenase (Bethyl Labs, Montgomery, TX), total and phosphorylated Akt (Ser 473), total and phosphorylated Erk 1/2 (pERK1/2) (Thr 202/Tyr 204), total and phosphorylated p70S6K (Thr 389), total RSK1/RSK2/RSK3 and phosphorylated RSK (Ser 380), total and phosphorylated PS6 (Ser 235/236), and PTEN (all Cell Signaling Technology).

Lung Histology, Immunostaining, and Total Lung Collagen

Lungs were inflation fixed using 4% paraformaldehyde and stained with hematoxylin and eosin as described previously (18). For immunohistochemical detection of proliferation, paraffin sections were immunostained with anti-mouse Ki67 antigen (Dako, Glostrup, Denmark). The total numbers of Ki67-staining nuclei were counted, as well as the total number of nuclei in 10 randomly selected uniform fields (26.2 mm^2) that encompassed alveolar, pleural, and adventitial regions of the lung for each mouse. The proliferation index was determined by counting the total number of Ki-67–staining nuclei and dividing by the total number of nuclei in each field. Total lung collagen was determined by quantifying total soluble collagen (Sircol Collagen Assay; Biocolor, Dublin, Ireland).

RNA Preparation and Real-Time PCR

Total RNA was extracted from lung tissue and cells using the RNeasy Mini Kit (Qiagen Sciences, Valencia, CA), as described previously (31). Real-time primer sequences for *hprt*, *Col1a*, *Col3a*, *Col5a*, and *Elastin* are provided in the supplementary MATERIALS AND METHODS section.

Pulmonary Mechanics

Lung mechanics were assessed on mice with a computerized Flexi Vent system (SCIREQ, Montreal, PQ, Canada), as previously described (33, 34).

Statistical Analysis

All data were analyzed with Prism (version 5; GraphPad Inc., La Jolla, CA). One-way ANOVA with Tukey's multiple comparison post test was used to compare different experimental groups, and data were considered statistically significant with *P* values less than 0.05.

RESULTS

Activation of ERK1/2 in the Lung Cells during TGF-α–Induced Pulmonary Fibrosis

CCSP/TGF-α mice were treated with Dox to induce TGF-α expression for 1 and 4 days. Induction of TGF-α caused increased pERK1/2 as measured by Western blot of whole-lung homogenate (Figures 1A) and quantified using the volume integration function on PhosphorImager software when comparing the ratio of pERK1/2 to total ERK1/2 ($P < 0.05$ versus CCSP/- control).

To investigate the cellular sources of ERK1/2 activity, immunofluorescence staining with anti-pERK1/2 antibody was performed on lung sections from CCSP/- and CCSP/TGF-α transgenic mice at 4 days on Dox when fibrosis was developing and at 4 weeks when fibrosis was established. In CCSP/TGF-α mice, pERK1/2 colocalized with α-SMA staining in the peribronchial and perivascular adventitia at 4 days and 4 weeks (Figure 1B), as well as in pleural fibrotic lesions at 4 weeks (Figure 1C). To characterize

ERK1/2 activation in epithelial cells, lung sections were stained with anti-CCSP (Figure 1D). In contrast to the myofibroblasts, pERK1/2 immunofluorescence was less prominent in airway epithelial cells in CCSP/TGF-α mice, suggesting that ERK1/2 activation is more dominant in mesenchymal cells compared with epithelial cells during TGF-α–induced pulmonary fibrosis. Colocalization of pERK1/2 with vimentin further supports ERK1/2 activation in lung mesenchymal cells of the lung during TGF-α–driven fibrosis (see Figure E1 in the online supplement). These immunofluorescence studies support a selective activation of MEK/ERK pathway in mesenchymal cells in CCSP/TGF-α transgenic mice in areas of developing and mature fibrotic lesions.

ARRY Selectively Inhibits TGF-α–Induced Phosphorylation of ERK1/2 in Fibroblasts

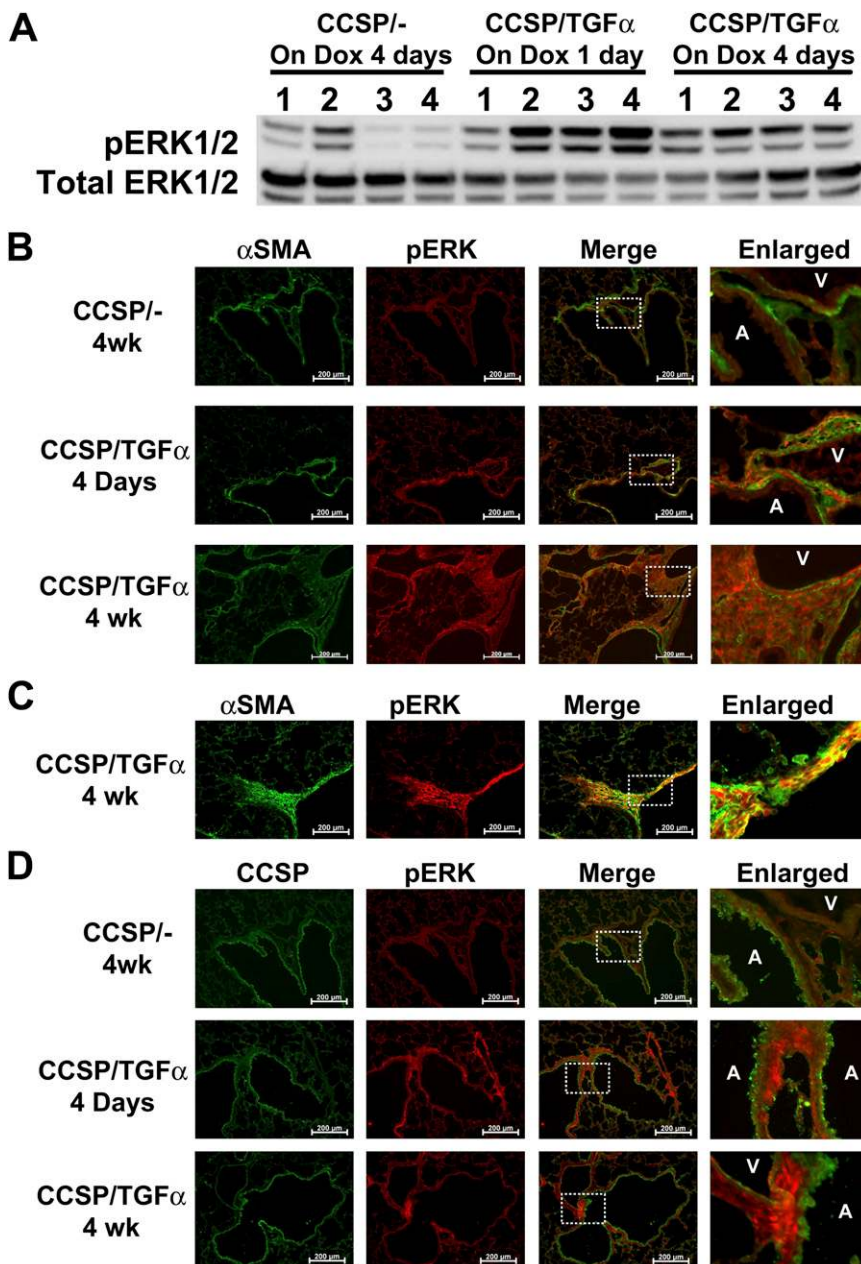To determine if TGF-α directly activates ERK1/2 in fibroblasts, primary lung fibroblasts were isolated from FVB/N

Figure 1. Phosphorylation of extracellular signal–regulated kinase ERK1/2 in the lung cells during transforming growth factor (TGF)-α–induced pulmonary fibrosis. (A) Clara cell–specific protein (CCSP)-rtTA$^{+/-}$ (CCSP/-) and CCSP-rtTA$^{+/-}$/(TetO)$_7$-cmv TGF-α$^{+/-}$ (CCSP/TGF-α) mice were on doxycycline (Dox) for 1 day or 4 days. Whole-lung cell extracts were prepared and 50 μg of protein were subjected to SDS-PAGE and Western blot analysis. Blots were probed with antibodies against the phosphorylated form of ERK (pERK1/2) and total ERK1/2. (B) Representative photomicrographs of lung tissues stained for pERK1/2 (red) and α-smooth muscle actin (α-SMA) (green). CCSP/- and CCSP/TGF-α mice were treated with Dox for 4 days or 4 weeks. Lungs were snap frozen and embedded in OCT. α-SMA, a marker for smooth muscle cells, was specifically stained only in the cells surrounding the large airways (A) and blood vessels (V). Overlaid and enlarged images show a colocalization of signals for pERK1/2 with α-SMA–positive cells, indicating that these pERK1/2-positive cells were mesenchymal cells. Scale bar, 200 μM. (C) Representative photomicrographs of lung plural regions stained for pERK1/2 (red) and α-SMA (green). α-SMA specifically stained the thickened pleural fibrotic regions of fibrotic lungs. Overlaid and enlarged images show a colocalization of signals for pERK1/2 with α-SMA–positive cells, indicating that these pERK1/2-positive cells were mesenchymal cells. Scale bar, 200 μM. (D) Representative photomicrographs of lung tissues stained for pERK1/2 (red) and CCSP (green). CCSP/- and CCSP/TGF-α mice were treated with Dox for 1 day or 4 weeks. CCSP, a marker for bronchiolar epithelial cells, was specifically stained only in the cells of airways. Overlaid and enlarged images show minimal colocalization between pERK1/2- and CCSP-positive cells. Airways and blood vessels are indicated by A and V, respectively. Scale bar, 200 μm. Images represent two independent fluorescence staining of lung tissues with similar results. (B–D) Dashed rectangles in third column (Merge) indicate the area shown in forth column (Enlarged).
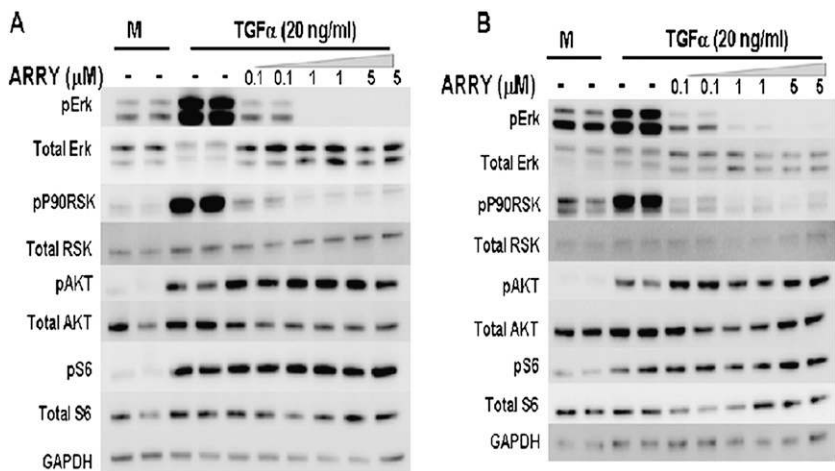
Figure 2. Inhibition of mitogen-activated protein kinase (MAPK)/ERK pathway in mouse and human lung primary fibroblasts using MAPK kinase (MEK)–specific inhibitor, ARRY-142886 (ARRY). (*A*) Collagenase-digested lungs from CCSP/- mice were cultured for 10 days to obtain primary fibroblasts as described in Materials and Methods. Serum-starved mouse primary fibroblasts were pretreated with 0.1, 5, and 10 μM ARRY for 30 minutes before stimulation with vehicle or TGF-α (20 ng/ml) for 30 minutes. Cells were lysed and analyzed by immunoblotting. Treatment with ARRY resulted in a dose-dependent inhibition of pERK1/2 and p90 ribosomal S6 kinase (p90RSK), but no effect on phosphorylation of AKT (pAKT) and S6K (pS6). (*B*) Serum-starved human primary fibroblasts were pretreated with ARRY for 30 minutes before stimulation with vehicle or TGF-α (20 ng/ml) for 30 minutes. As in mouse fibroblasts, treatment with ARRY resulted in a dose-dependent inhibition of pERK1/2 and p90RSK, but no effect on pAKT or pS6. Equal loading is confirmed using glyceraldehyde 3-phosphate dehydrogenase (GAPDH) antibody staining. For the gels illustrated in this figure, phosphorylated and total proteins were run on the same samples on separate gels under the same conditions and are combined for illustrative purposes.

CCSP/- mice and stimulated with TGF-α. Cell signaling intermediates downstream of EGFR were then measured from fibroblast cell lysates without and with incubation of the MEK pharmacological inhibitor, ARRY. TGF-α added to fibroblasts directly induced phosphorylation of Erk and the downstream substrate, P90RSK (Figure 2A). TGF-α also induced activation of the PI3K pathway, evident by phosphorylation of Akt, as well as the mTOR downstream substrate, pS6.
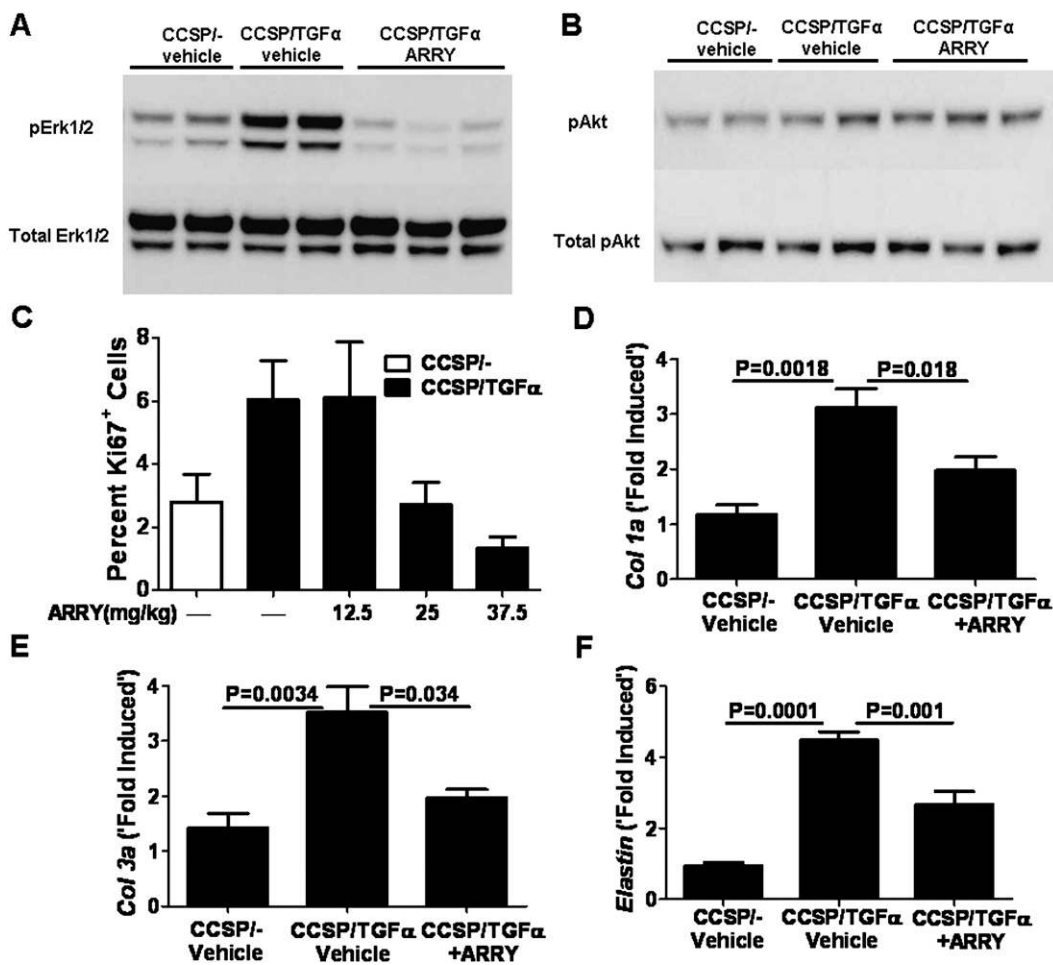

Figure 3. Effect of *in vivo* inhibition of ERK1/2 phosphorylation using MEK-specific inhibitor, ARRY, attenuates TGF-α–induced lung cell proliferation and expression of matrix genes. Effect of ARRY on ERK (*A*) and Akt (*B*) phosphorylations. CCSP/- and CCSP/TGF-α mice on Dox for 4 days were cotreated with vehicle or ARRY (12.5 mg/kg twice daily). Total lung lysates were analyzed by immunoblotting. Treatment with ARRY inhibited pERK1/2, but had no effect on pAKT. For the gels illustrated in this figure, phosphorylated and total proteins were run on the same samples on separate gels under the same conditions and are combined for illustrative purposes. (*C*) Effect of ARRY on lung cell proliferation. CCSP/- and CCSP/TGF-α mice on Dox for 4 days were cotreated with vehicle or different doses of ARRY (12.5, 25, and 37.5 mg/kg twice daily). Proliferation was assessed at Day 4 using immunohistochemistry for the proliferation marker, Ki67. Data are percent of Ki67 cells per total lung cells in randomly counted lung fields. Data shown are mean values (±SEM). (*D–F*) Effect of ARRY on expression of extracellular matrix genes, *col1a*, *col3a*, and *elastin*. Real-time PCR analysis was performed in the lungs of CCSP/- and CCSP/TGF-α mice on Dox for 4 days and treated with vehicle or ARRY (37.5 mg/kg twice daily) for 4 days. The fold change was obtained by normalizing the gene expression number to those of HPRT, then comparing the samples to the CCSP/- mice treated with vehicle for 4 days. Data shown are mean values (±SEM) (*n* = 6–10/group). Statistical significance for data was measured using one-way ANOVA (*n* = 4–5/group).

Incubation of fibroblasts with ARRY prevented phosphorylation of ERK1/2, while not inhibiting phosphorylation of Akt or S6. Studies were repeated in normal adult human lung fibroblasts incubated with TGF-α with patterns of signaling intermediate phosphorylation and inhibition with ARRY alike to mouse lung fibroblasts (Figure 2B). These *in vitro* fibroblast studies demonstrate that TGF-α directly activates the MEK pathway with signaling conserved between mouse and human fibroblasts. ARRY selectively inhibits Erk phosphorylation in fibroblasts without altering phosphorylation of PI3K or mTOR downstream intermediates.

MEK Inhibition Prevents TGF-α–Induced Lung Cell Proliferation and Matrix Gene Production *In Vivo*

CCSP/TGF-α mice were treated *in vivo* with either ARRY (12.5 mg/kg twice per day) or vehicle while concomitantly administering Dox to induce TGF-α expression. Mice were killed after 4 days of Dox, and lungs were homogenized to measure phosphorylation of ERK1/2 and Akt. Mice treated with ARRY demonstrated inhibition of ERK1/2 phosphorylation with no changes in phosphorylation of Akt (Figures 3A and 3B). These studies demonstrate that ARRY selectively inhibits ERK1/2 phosphorylation *in vivo* without altering Akt phosphorylation.

Previous preclinical oncology studies in mice used proliferation with Ki67 staining as the method to verify adequate dosing regimens (35). We previously demonstrated that activation of TGF-α for 4 days was sufficient to increase the proliferation of mesenchymal and epithelial cells (7). Therefore, to determine if modulation of Erk phosphorylation is associated with physiologic changes of fibroproliferation, we measured proliferation with Ki67 staining in CCSP/TGF-α mice after 4 days of Dox administration with ARRY treatment. Compared with CCSP/TGF-α mice treated with vehicle, proliferation was unchanged in mice treated with ARRY at 12.5 mg/kg twice daily, whereas higher doses of 25 and 37.5 mg/kg twice daily inhibited proliferation (Figure 3C). To assess the efficacy of ARRY at inhibiting lung matrix gene expression at the higher dose (37.5 mg/kg), RT-PCR for collagen 1a, collagen 3a, and elastin were also performed on lung homogenates on mice receiving 4 days of both Dox and ARRY (37.5 mg twice daily). ARRY administration significantly attenuated increased transcript levels for the matrix genes compared with vehicle-treated controls (Figures 3D–3F). These studies demonstrate that inhibition of the MEK pathway in a dose–response manner is sufficient to prevent TGF-α–induced proliferation, as well as matrix gene expression. The inability of the 12.5 mg/kg dose to inhibit proliferation is likely due to the short half-life of ARRY (8 h) (35), and is consistent with previous preclinical tumor xenograft studies, which found doses in the 25–50 mg/kg of body weight range sufficient to sustain Erk inhibition (36, 37). The ensuing MEK inhibition studies used ARRY at a dose of 37.5 mg/kg twice daily to ensure Erk inhibition was sustained during the 12-hour dosing interval.
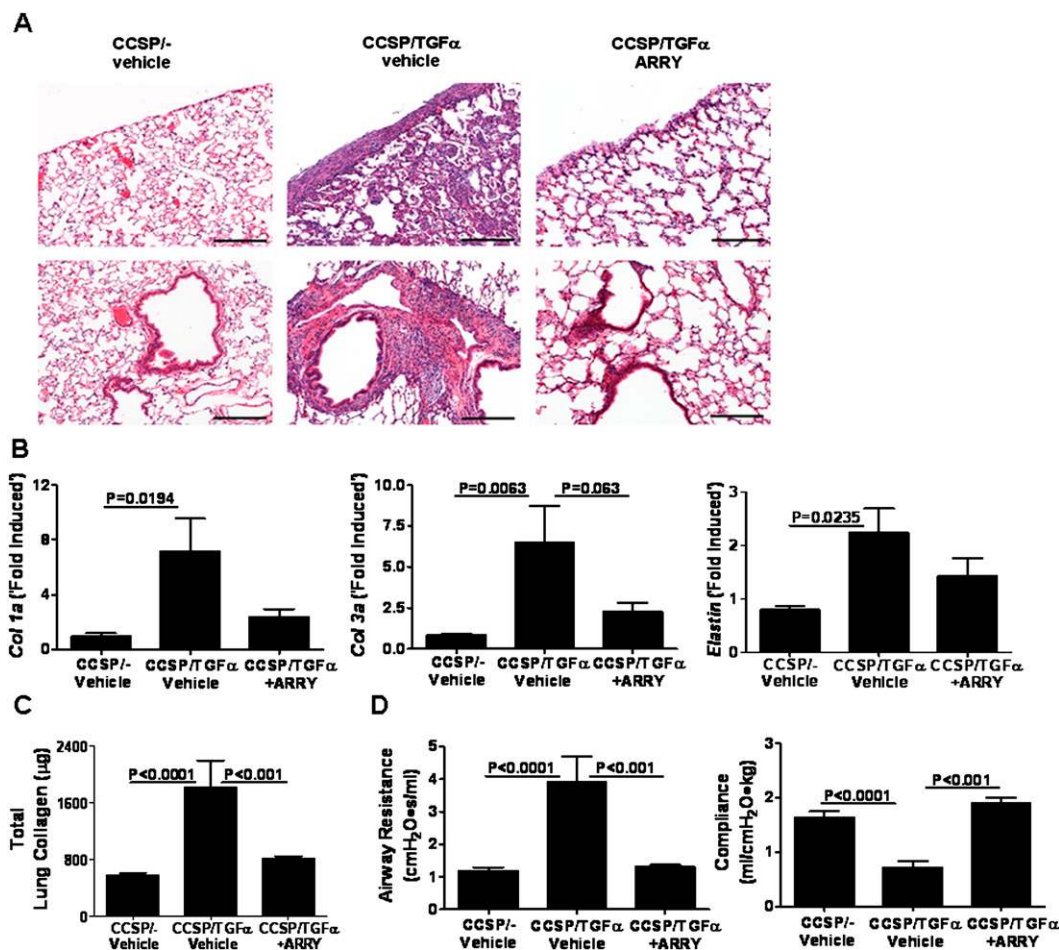

Figure 4. Prevention of TGF-α–induced pulmonary fibrosis by ARRY. CCSP/- and CCSP/TGF-α mice on Dox were treated with vehicle or ARRY (37.5 mg/kg twice daily) for 4 weeks. CCSP/TGF-α mice administered ARRY at the initiation of TGF-α induction demonstrated marked attenuation of fibrosis as compared with vehicle-treated CCSP/TGF-α mice. (*A*) Representative photomicrographs of lung tissues for each group stained with hematoxylin and eosin (H&E) and taken at 10× magnification. *Upper panel* shows the area of airways, vessels, and parenchyma of the lung. *Lower panel* shows the pleural regions of the lung. *Scale bar,* 200 μm. (*B*) ARRY administered at the time of TGF-α induction prevented expression of extracellular matrix genes, *col1a, col3a,* and *elastin.* Real-time PCR analysis was performed using total lung RNA isolated from the lungs of CCSP/- and CCSP/TGF-α mice. Data are means (±SEM) (*n = 5/*group). (*C*) ARRY administered at the time of TGF-α induction prevented increases in total lung collagen. Data are means (±SEM) (*n = 7–10/*group). (*D*) ARRY administered at the time of TGF-α induction prevented increases in airway resistance and compliance compared with vehicle-treated CCSP/TGF-α transgenic mice receiving 4 weeks of Dox. Data are means (±SEM) (*n = 7–10/*group). Statistical significance between groups was measured using one-way ANOVA.

MEK Inhibition Prevents TGF-α–Induced Pulmonary Fibrosis

To determine if MEK inhibition prevents the physiologic consequences of progressive lung fibrosis, CCSP/TGF-α mice were treated with Dox to induce TGF-α expression and concomitantly treated with either ARRY (37.5 mg/kg) or vehicle twice per day for 4 weeks and compared with CCSP/- nonfibrotic control mice. Induction of TGF-α caused extensive pleural, perivascular, and peribronchial fibrosis on lung histology, whereas CCSP/TGF-α mice treated with ARRY demonstrated no fibrosis (Figure 4A). RT-PCR for collagen 1a, collagen 3a, and elastin from lung homogenates revealed a marked increases in transcripts in CCSP/TGF-α mice administered vehicle, with significant blunting of transcript changes in ARRY-treated mice (Figure 4B). In agreement with the transcriptional changes, total lung collagen levels were over threefold higher in CCSP/TGF-α mice compared with Dox-treated CCSP/- control mice, with collagen levels significantly reduced in ARRY treated mice (Figure 4C). Lung compliance decreased by over 50%, and airway resistance increased threefold in CCSP/TGF-α vehicle–treated mice compared with CCSP/- control mice, whereas CCSP/TGF-α mice treated with ARRY did not show any differences in lung mechanics compared with CCSP/- control mice (Figure 4D). Together, these studies demonstrate that inhibition of MEK at the time of TGF-α overexpression prevents collagen accumulation and changes in lung mechanics.

MEK Inhibition Prevents Progression of Established Pulmonary Fibrosis

To determine whether MEK inhibition influences the progression of established fibrosis, after 4 weeks of Dox treatment when fibrosis is already manifest, CCSP/TGF-α mice were administered ARRY while remaining on Dox for an additional 4 weeks (8 wk total) (Figure 5A). Controls included CCSP/- and CCSP/TGF-α mice treated with vehicle while remaining on Dox for an additional 4 weeks. Body weights of CCSP/TGF-α mice treated with vehicle decreased 35% from baseline after 8 weeks of Dox (Figure 5B). ARRY administered at the beginning of Week 5 decelerated body weight loss compared with vehicle-treated CCSP/TGF-α mice, with body weights remaining lower than CCSP/- control mice. At the initiation of the study, there were 8 mice in the CCSP/- control group, 10 mice in the CCSP/TGF-α vehicle group, and 9 mice in the CCSP/TGF-α ARRY–treated group. No deaths occurred in either the controls or ARRY-treated group, with three deaths in the vehicle-treated CCSP/TGF-α mice on Dox. However, two of the three deaths in this group were unrelated to the fibrosis (cage malfunctions), and occurred early in the study before fibrosis became prominent. There were no differences in mortality among the groups adjusting for the unrelated deaths in the vehicle-treated group.

CCSP/TGF-α mice treated with Dox and vehicle for 8 weeks demonstrated manifest pleural thickening with advanced perivascular and peribronchial fibrosis affecting large and small vessels and airways (Figure 6A). CCSP/TGF-α mice treated with ARRY demonstrated reduced pleural fibrosis, as well as reduced perivascular and peribronchial fibrosis, compared with vehicle-treated mice (Figure 6A). RT-PCR for collagen 1a, collagen 3a, and collagen 5a from lung homogenates demonstrated increases in transcripts for CCSP/TGF-α mice administered vehicle, with significant attenuation of transcript changes in ARRY-treated mice (Figure 6B). Total lung collagen demonstrated significantly increased collagen in CCSP/TGF-α mice treated with vehicle or ARRY, with no differences detected between the latter two groups (Figure 6C). The discrepancy in lung collagen measured by RT-PCR and seen on lung histology
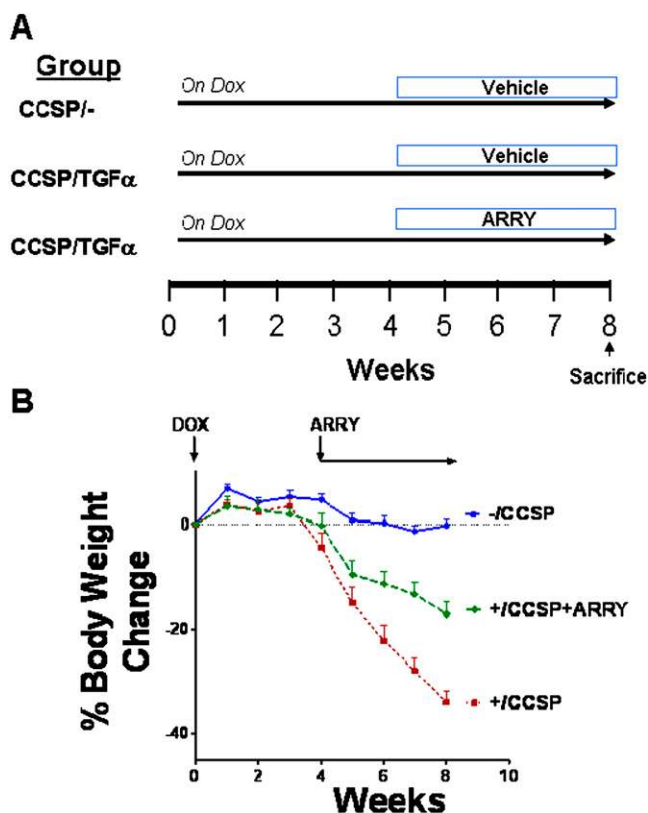

Figure 5. ARRY prevents progressive weight loss during TGF-α–induced fibrosis. To assess the efficacy of phosphatidylinositol 3-kinase (PI3K) inhibition in established fibrosis, CCSP/TGF-α transgenic mice were treated with ARRY after 4 weeks of Dox, while remaining on Dox for an additional 4 weeks. (*A*) The treatment protocol is represented schematically. Controls included CCSP/- and CCSP/TGF-α mice treated with vehicle while remaining on Dox an additional 4 weeks. Mice were weighed weekly during treatments as described in MATERIALS AND METHODS. (*B*) Dox-induced expression of TGF-α for 8 weeks caused progressive weight loss in vehicle-treated mice (*red line*), whereas mice treated with ARRY 4 weeks after TGF-α induction did not have changes in body weight (*green line*), but weights remained below CCSP/- controls (*blue line*). No change in bodyweight of mice is represented as 0%. Data are means (±SEM) and statistical significance between groups was measured using one-way ANOVA (*n* = 7–9/group).

likely reflects the limitations of the Sircol assay, which detects only soluble collagen and cannot detect aged covalent cross-linked insoluble collagen, which would be more prevalent in the vehicle-treated mice. Treatment of CCSP/TGF-α mice with Dox and vehicle for 8 weeks caused significant changes in the lung mechanics compared with CCSP/- mice (Figure 6D). When ARRY was administered at the beginning of Week 5, CCSP/TGF-α transgenic mice exhibited reduced increases in airway resistance and decreased compliance (Figure 6D). Together, these studies demonstrate that MEK inhibition administered at the time of extensive and established fibrosis modulates the progression of disease based on physiologic and histologic parameters.

DISCUSSION

The present study provides three novel insights in the TGF-α lung fibrosis model: (*1*) pharmacologic MEK inhibition prevents the evolution of fibrosis that is already embedded and progressing;
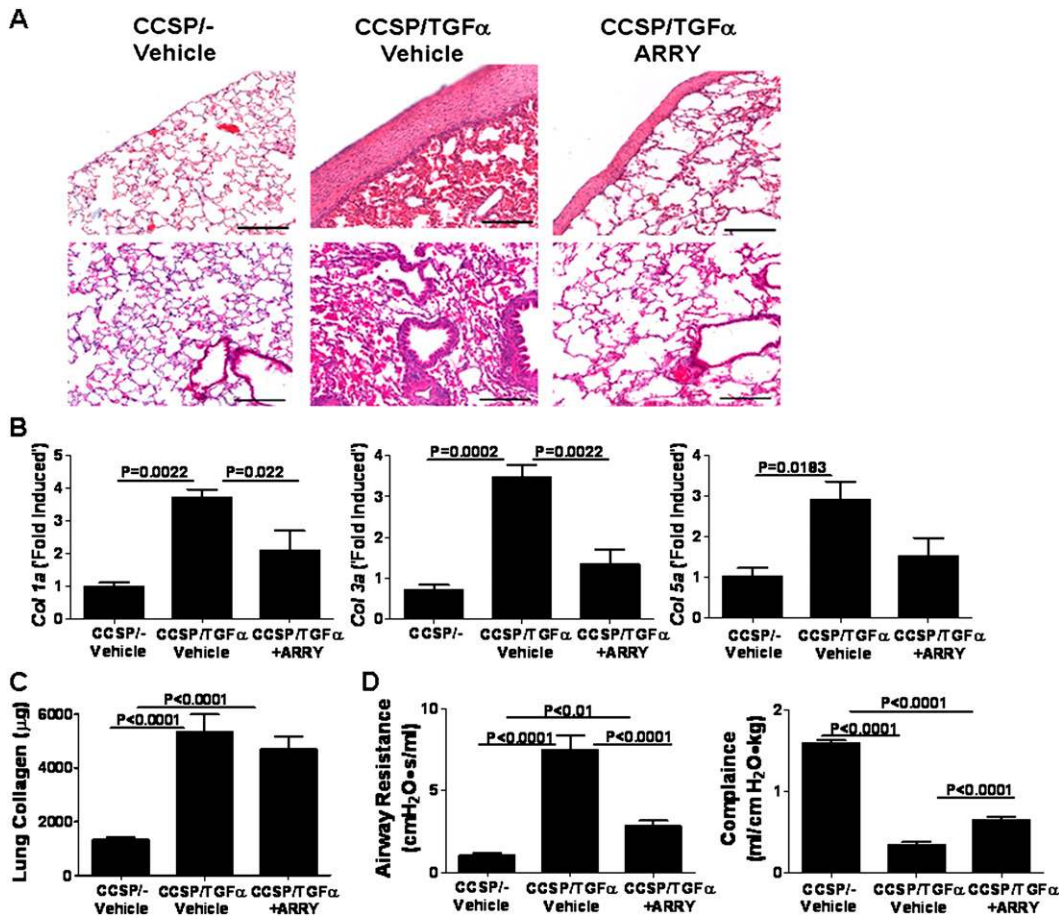
Figure 6. ARRY attenuates progression of lung fibrosis. (*A*) Representative photomicrographs of lung tissues for each group stained with H&E and taken at 10× magnification. *Upper panel* shows the area of airways, vessels, and parenchyma of the lung. *Lower panel* shows the pleural regions of the lung. *Scale bar*, 200 μm. (*B*) ARRY administered 4 weeks after the initiation of TGF-α induction demonstrated attenuation of transcripts for extracellular matrix genes, *col1a*, *col3a*, and *col5a*. Real-time PCR analysis was performed using total lung RNA isolated from the lungs. Data are means (±SEM) ($n = 4$/group). (*C*) ARRY administered 4 weeks after the initiation of TGF-α induction demonstrated no change in total lung collagen compared with vehicle-treated mice. Data are means (±SEM) ($n = 7–9$/group). (*D*) ARRY prevents progression of TGF-α–dependent changes in lung mechanics. CCSP/TGF-α transgenic mice administered ARRY 4 weeks after treatment with Dox demonstrated reduced increases in airway resistance and compliance as compared with vehicle-treated CCSP/TGF-α transgenic mice receiving 8 weeks of Dox. Data are means (±SEM) and statistical significance between groups was measured using one-way ANOVA ($n = 7–9$/group).

(2) inhibition of the MEK pathway prevents fibrosis independent of persistent PI3K activation; and (3) MEK/ERK is primarily activated in mesenchymal cells of fibrotic lesions.

Using biochemical, histologic, and physiologic methods, our data demonstrate that MEK inhibition prevented the progression of established disease when administered as a rescue therapy. To our knowledge, this is the first study to successfully demonstrate that inhibition of the MEK/ERK pathway *in vivo* attenuates the progression of fibrosis and physiologic alterations in lung mechanics. The clinical relevance for this finding is the strong evidence demonstrating up-regulation of ERK/MAPK in human fibrotic disease (38, 39). Yoshida and colleagues (39) analyzed transcripts for Akt and MAPK signaling pathways in lung tissue of patients with idiopathic pulmonary fibrosis (IPF), and found increased levels of serine/threonine-protein kinase B-Raf (BRAF) compared with normal lung control subjects. BRAF is a major signaling intermediate protein that regulates the MAPK/ERK pathway. Western blot of human lung biopsy samples also demonstrates increased ERK1/2 signaling in IPF samples compared with normal lungs (38). The recent development of pharmacologic inhibitors of MAPK/ERK that are in clinical oncology trials, coupled with the findings of this study, support additional studies in animal models and humans to verify MAPK/ERK as a therapeutic target in fibrotic disease.

We previously demonstrated that inhibition of the PI3K/Akt pathway with the specific PI3K inhibitor, PX-866, prevented fibrosis in the CCSP/TGF-α model, despite unaltered activation of the MAPK/ERK pathway (18). In the current study, Akt remained phosphorylated both *in vitro* and *in vivo* (Figures 2 and 3B) after

TGF-α induction, confirming the specificity of ARRY inhibition. The effectiveness of either PX-866 or ARRY in preventing fibrosis development suggests that inhibition of either the PI3K or MEK/ERK pathway is sufficient to prevent significant fibrosis from becoming established. Together, these findings would suggest that both pathways need to be active *in vivo* to induce fibroproliferation, but the mechanism for this observation remains under investigation. One possible explanation for these findings includes cell-selective pathway activation. We previously demonstrated Akt phosphorylation primarily in airway and type II epithelial cells after TGF-α induction (40). In contrast, we observed elevated ERK activity primarily in α-SMA and vimentin-positive mesenchymal cells of lungs from CCSP/TGF-α mice on Dox for 4 days or 4 weeks (Figure 1). Interestingly, similar to the CCSP/TGF-α model, immunohistochemistry of human lung sections from patients with IPF demonstrates increased pERK1/2, primarily in smooth muscle cells, with little activation in the epithelium (41). An alternative explanation includes a common converging pathway downstream of both PI3K and MAPK/ERK, whereby input from both pathways is required for activation. The mTOR is a highly conserved intracellular serine/threonine kinase and a major downstream component of the PI3K pathway (42). Activation of mTOR, in complex with raptor (mTORC1), leads to phosphorylation of p70S6K and 4E-binding proteins (4E-BPs) (43, 44). p70S6K and 4E-BPs control the translation of specific mRNAs and protein synthesis involved in cell cycle regulation, with effects on cellular growth, proliferation, and translation (44). The p70S6K and 4E-BP pathways possess several phosphorylation sites that are points

of convergence not only for mTORC1, but also for MAPK (43, 44). Together, these findings provide a basis to further investigate molecular events and downstream targets in both the PI3K and MEK/ERK pathways that contribute to pulmonary fibrosis initiation.

CCSP/TGF-α mice administered ARRY as a rescue therapy 4 weeks after beginning Dox demonstrated significant improvements with 4 weeks of treatment in lung histology, lung mechanics, body weights, and collagen gene transcripts compared with vehicle-treated mice, demonstrating that Erk inhibition prevented the progression of fibrosis. However, all parameters remained altered compared with control mice. We previously reported that fibrosis in the CCSP/TGF-α model is completely reversible when TGF-α overexpression is extinguished after 4 weeks of induction (18). Therefore, if ARRY was successful in completely reversing the fibrosis, endpoints in the ARRY-treated rescue group would be expected to return to no fibrosis/control levels. As all endpoints in the ARRY-treated group remained above the control values, these findings demonstrate that prevention of fibrosis does not guarantee reversal once the fibrotic process is initiated. Further resolution of existing fibrosis may have required longer treatment times than 4 weeks. Alternatively, once fibrosis is established and progressing, multiple signaling pathways are likely activated and contribute toward the maintenance of lung fibrosis. We previously demonstrated that TGF-β1 is not activated during the induction of fibrosis in the CCSP/TGF-α model, but is detected in advanced fibrotic lesions (7). Therefore, inhibition of multiple pathways, such as TGF-β, may be required to accelerate or complete fibrosis resolution. The concept of combined signaling pathway inhibition has proved effective in transgenic and xenograft models of cancer (45–47), and our findings support that the resolution of existing and progressing fibroproliferative diseases is likely complex, involving multiple pathways.

In summary, overexpression of TGF-α in the lung epithelium is associated with mesenchymal cell activation of the MEK/ERK signaling pathway. There are strong data supporting activation of ERK in human fibrotic disease, and the MEK/ERK pathway is a logical target for potential fibrosis therapy, as several fibrogenic cytokines signal through MEK/ERK, including noncanonical TGF-β, platelet-derived growth factor, IL-13, and TNF-α (14, 48). In addition, cell cycle progression in lung mesenchymal cells is regulated through ERK1/2 by altering expression of cyclin D1 and CDK4 (49). In the TGF-α model, selective inhibition of MEK prevented the development of fibrosis and attenuated the progression of fibrosis when administered as a rescue therapy. These findings support the concept that MEK/ERK activation may play a significant role in human lung fibrotic disease, which could be amenable to targeted therapy.

References

1. Hardie WD, Glasser SW, Hagood JS. Emerging concepts in the pathogenesis of lung fibrosis. *Am J Pathol* 2009;175:3–16.
2. Wynn TA. Cellular and molecular mechanisms of fibrosis. *J Pathol* 2008; 214:199–210.
3. Madala SK, Maxfield MD, Davidson CR, Schmidt SM, Garry D, Ikegami M, Hardie WD, Glasser SW. Rapamycin regulates bleomycin-induced lung damage in SP-C–deficient mice. *Pulm Med* 2011;2011: 653524.
4. Thannickal VJ, Toews GB, White ES, Lynch JP III, Martinez FJ. Mechanisms of pulmonary fibrosis. *Annu Rev Med* 2004;55:395–417.
5. Raghu G, Collard HR, Egan JJ, Martinez FJ, Behr J, Brown KK, Colby TV, Cordier JF, Flaherty KR, Lasky JA, *et al.* An official ATS/ERS/JRS/ALAT statement: idiopathic pulmonary fibrosis: evidence-based guidelines for diagnosis and management. *Am J Respir Crit Care Med* 2011;183:788–824.
6. Crystal RG, Bitterman PB, Mossman B, Schwarz MI, Sheppard D, Almasy L, Chapman HA, Friedman SL, King TE Jr, Leinwand LA, *et al.* Future research directions in idiopathic pulmonary fibrosis: summary of a National Heart, Lung, and Blood Institute working group. *Am J Respir Crit Care Med* 2002;166:236–246.
7. Hardie WD, Le Cras TD, Jiang K, Tichelaar JW, Azhar M, Korfhagen TR. Conditional expression of transforming growth factor-alpha in adult mouse lung causes pulmonary fibrosis. *Am J Physiol Lung Cell Mol Physiol* 2004;286:L741–L749.
8. Lee CG, Kang HR, Homer RJ, Chupp G, Elias JA. Transgenic modeling of transforming growth factor-beta(1): role of apoptosis in fibrosis and alveolar remodeling. *Proc Am Thorac Soc* 2006;3:418–423.
9. Yoshida M, Sakuma J, Hayashi S, Abe K, Saito I, Harada S, Sakatani M, Yamamoto S, Matsumoto N, Kaneda Y, *et al.* A histologically distinctive interstitial pneumonia induced by overexpression of the interleukin 6, transforming growth factor beta 1, or platelet-derived growth factor b gene. *Proc Natl Acad Sci USA* 1995;92:9570–9574.
10. Sato S, Nagaoka T, Hasegawa M, Tamatani T, Nakanishi T, Takigawa M, Takehara K. Serum levels of connective tissue growth factor are elevated in patients with systemic sclerosis: association with extent of skin sclerosis and severity of pulmonary fibrosis. *J Rheumatol* 2000;27: 149–154.
11. Wilson MS, Madala SK, Ramalingam TR, Gochuico BR, Rosas IO, Cheever AW, Wynn TA. Bleomycin and IL-1beta-mediated pulmonary fibrosis is IL-17a dependent. *J Exp Med* 2010;207:535–552.
12. Mentink-Kane MM, Wynn TA. Opposing roles for IL-13 and IL-13 receptor alpha 2 in health and disease. *Immunol Rev* 2004;202:191–202.
13. Chapman HA. Epithelial–mesenchymal interactions in pulmonary fibrosis. *Annu Rev Physiol* 2011;73:413–435.
14. Hardie WD, Hagood JS, Dave V, Perl AK, Whitsett JA, Korfhagen TR, Glasser S. Signaling pathways in the epithelial origins of pulmonary fibrosis. *Cell Cycle* 2010;9:2769–2776.
15. Kubiak J, Mitra MM, Steve AR, Hunt JD, Davies P, Pitt BR. Transforming growth factor-alpha gene expression in late-gestation fetal rat lung. *Pediatr Res* 1992;31:286–290.
16. Polosa R, Prosperini G, Leir SH, Holgate ST, Lackie PM, Davies DE. Expression of C-ERBB receptors and ligands in human bronchial mucosa. *Am J Respir Cell Mol Biol* 1999;20:914–923.
17. Vermeer PD, Einwalter LA, Moninger TO, Rokhlina T, Kern JA, Zabner J, Welsh MJ. Segregation of receptor and ligand regulates activation of epithelial growth factor receptor. *Nature* 2003;422:322–326.
18. Le Cras TD, Korfhagen TR, Davidson C, Schmidt S, Fenchel M, Ikegami M, Whitsett JA, Hardie WD. Inhibition of PI3K by PX-866 prevents transforming growth factor-alpha–induced pulmonary fibrosis. *Am J Pathol* 2010;176:679–686.
19. Srinivasan M, Jewell SD. Evaluation of TGF-alpha and EGFR expression in oral leukoplakia and oral submucous fibrosis by quantitative immunohistochemistry. *Oncology* 2001;61:284–292.
20. Kohri K, Ueki IF, Nadel JA. Neutrophil elastase induces mucin production by ligand-dependent epidermal growth factor receptor activation. *Am J Physiol Lung Cell Mol Physiol* 2002;283:L531–L540.
21. Madtes DK, Raines EW, Sakariassen KS, Assoian RK, Sporn MB, Bell GI, Ross R. Induction of transforming growth factor-alpha in activated human alveolar macrophages. *Cell* 1988;53:285–293.
22. Wang X, Huong SM, Chiu ML, Raab-Traub N, Huang ES. Epidermal growth factor receptor is a cellular receptor for human cytomegalovirus. *Nature* 2003;424:456–461.
23. Gallucci RM, Simeonova PP, Toriumi W, Luster MI. TNF-alpha regulates transforming growth factor-alpha expression in regenerating murine liver and isolated hepatocytes. *J Immunol* 2000;164:872–878.

24. Hardie WD, Korfhagen TR, Sartor MA, Prestridge A, Medvedovic M, Le Cras TD, Ikegami M, Wesselkamper SC, Davidson C, Dietsch M, *et al.* Genomic profile of matrix and vasculature remodeling in TGF-α–induced pulmonary fibrosis. *Am J Respir Cell Mol Biol* 2007;37: 309–321.

25. Bogdan S, Klambt C. Epidermal growth factor receptor signaling. *Curr Biol* 2001;11:R292–R295.

26. Hardie WD, Davidson C, Ikegami M, Leikauf GD, Le Cras TD, Prestridge A, Whitsett JA, Korfhagen TR. EGF receptor tyrosine kinase inhibitors diminish transforming growth factor-alpha–induced pulmonary fibrosis. *Am J Physiol Lung Cell Mol Physiol* 2008;294: L1217–L1225.

27. McCubrey JA, Steelman LS, Chappell WH, Abrams SL, Wong EW, Chang F, Lehmann B, Terrian DM, Milella M, Tafuri A, *et al.* Roles of the RAF/MEK/ERK pathway in cell growth, malignant transformation and drug resistance. *Biochim Biophys Acta* 2007;1773:1263–1284.

28. Xu SW, Howat SL, Renzoni EA, Holmes A, Pearson JD, Dashwood MR, Bou-Gharios G, Denton CP, du Bois RM, Black CM, *et al.* Endothelin-1 induces expression of matrix-associated genes in lung fibroblasts through MEK/ERK. *J Biol Chem* 2004;279:23098–23103.

29. Yeh TC, Marsh V, Bernat BA, Ballard J, Colwell H, Evans RJ, Parry J, Smith D, Brandhuber BJ, Gross S, *et al.* Biological characterization of ARRY-142886 (AZD6244), a potent, highly selective mitogen-activated protein kinase kinase 1/2 inhibitor. *Clin Cancer Res* 2007; 13:1576–1583.

30. Tichelaar JW, Lu W, Whitsett JA. Conditional expression of fibroblast growth factor-7 in the developing and mature lung. *J Biol Chem* 2000; 275:11858–11864.

31. Madala SK, Pesce JT, Ramalingam TR, Wilson MS, Minnicozzi S, Cheever AW, Thompson RW, Mentink-Kane MM, Wynn TA. Matrix metalloproteinase 12-deficiency augments extracellular matrix degrading metalloproteinases and attenuates IL-13–dependent fibrosis. *J Immunol* 2010;184:3955–3963.

32. Moore BB, Kolodsick JE, Thannickal VJ, Cooke K, Moore TA, Hogaboam C, Wilke CA, Toews GB. CCR2-mediated recruitment of fibrocytes to the alveolar space after fibrotic injury. *Am J Pathol* 2005; 166:675–684.

33. Schuessler TF, Bates JH. A computer-controlled research ventilator for small animals: design and evaluation. *IEEE Trans Biomed Eng* 1995; 42:860–866.

34. Hokuto I, Ikegami M, Yoshida M, Takeda K, Akira S, Perl AK, Hull WM, Wert SE, Whitsett JA. STAT-3 is required for pulmonary homeostasis during hyperoxia. *J Clin Invest* 2004;113:28–37.

35. Adjei AA, Cohen RB, Franklin W, Morris C, Wilson D, Molina JR, Hanson LJ, Gore L, Chow L, Leong S, *et al.* Phase I pharmacokinetic and pharmacodynamic study of the oral, small-molecule mitogen-activated protein kinase kinase 1/2 inhibitor AZD6244 (ARRY-142886) in patients with advanced cancers. *J Clin Oncol* 2008;26: 2139–2146.

36. Haass NK, Sproesser K, Nguyen TK, Contractor R, Medina CA, Nathanson KL, Herlyn M, Smalley KS. The mitogen-activated protein/extracellular signal–regulated kinase kinase inhibitor AZD6244

(ARRY-142886) induces growth arrest in melanoma cells and tumor regression when combined with docetaxel. *Clin Cancer Res* 2008;14: 230–239.

37. Shannon AM, Telfer BA, Smith PD, Babur M, Logie A, Wilkinson RW, Debray C, Stratford IJ, Williams KJ, Wedge SR. The mitogen-activated protein/extracellular signal–regulated kinase kinase 1/2 inhibitor AZD6244 (ARRY-142886) enhances the radiation responsiveness of lung and colorectal tumor xenografts. *Clin Cancer Res* 2009;15:6619–6629.

38. Antoniou KM, Margaritopoulos GA, Soufla G, Symvoulakis E, Vassalou E, Lymbouridou R, Samara KD, Kappou D, Spandidos DA, Siafakas NM. Expression analysis of Akt and MAPK signaling pathways in lung tissue of patients with idiopathic pulmonary fibrosis (IPF). *J Recept Signal Transduct Res* 2010;30:262–269.

39. Yoshida K, Kuwano K, Hagimoto N, Watanabe K, Matsuba T, Fujita M, Inoshima I, Hara N. MAP kinase activation and apoptosis in lung tissues from patients with idiopathic pulmonary fibrosis. *J Pathol* 2002;198:388–396.

40. Korfhagen TR, Le Cras TD, Davidson CR, Schmidt SM, Ikegami M, Whitsett JA, Hardie WD. Rapamycin prevents transforming growth factor-α–induced pulmonary fibrosis. *Am J Respir Cell Mol Biol* 2009; 41:562–572.

41. Appleton CT, Usmani SE, Mort JS, Beier F. Rho/ROCK and MEK/ERK activation by transforming growth factor-alpha induces articular cartilage degradation. *Lab Invest* 2010;90:20–30.

42. Hartford CM, Ratain MJ. Rapamycin: something old, something new, sometimes borrowed and now renewed. *Clin Pharmacol Ther* 2007;82: 381–388.

43. Dann SG, Selvaraj A, Thomas G. mTOR complex1-S6K1 signaling: at the crossroads of obesity, diabetes and cancer. *Trends Mol Med* 2007; 13:252–259.

44. Dowling RJ, Topisirovic I, Alain T, Bidinosti M, Fonseca BD, Petroulakis E, Wang X, Larsson O, Selvaraj A, Liu Y, *et al.* mTORC1-mediated cell proliferation, but not cell growth, controlled by the 4E-BPS. *Science* 2010;328:1172–1176.

45. Engelman JA, Chen L, Tan X, Crosby K, Guimaraes AR, Upadhyay R, Maira M, McNamara K, Perera SA, Song Y, *et al.* Effective use of PI3K and MEK inhibitors to treat mutant KRAS G12D and PIK3CA H1047R murine lung cancers. *Nat Med* 2008;14:1351–1356.

46. Downward J. Targeting RAS and PI3K in lung cancer. *Nat Med* 2008;14: 1315–1316.

47. Li D, Shimamura T, Ji H, Chen L, Haringsma HJ, McNamara K, Liang MC, Perera SA, Zaghlul S, Borgman CL, *et al.* Bronchial and peripheral murine lung carcinomas induced by T790M-L858R mutant EGFR respond to HKI-272 and rapamycin combination therapy. *Cancer Cell* 2007;12:81–93.

48. Kim S, Shim JJ, Burgel PR, Ueki IF, Dao-Pick T, Tam DC, Nadel JA. IL-13–induced Clara cell secretory protein expression in airway epithelium: role of EGFR signaling pathway. *Am J Physiol Lung Cell Mol Physiol* 2002;283:L67–L75.

49. Jia X, Liu B, Shi X, Ye M, Zhang F, Liu H. Roles of the ERK, JNK/AP-1/cyclin D1–CDK4 pathway in silica-induced cell cycle changes in human embryo lung fibroblast cells. *Cell Biol Int* 2011;35:697–704.